Supine to upright lung mechanics: Do changes in lung shape influence lung tissue deformation?

Ho-Fung Chan, Merryn H. Tawhai, David L. Levin, Brian B. Bartholmai, Alys R. Clark

Abstract— **In this study we analyze lung shape change between the upright and supine postures and the effect of this shape change on the deformation of lung tissue under gravity. We use supine computed tomography images along with upright tomosynthesis images obtained on the same day to show that there is significant diaphragmatic movement between postures. Using a continuum model of lung tissue deformation under gravity we show that the shape changes due to this diaphragmatic movement could result in different lung tissue expansion patterns between supine and upright lungs. This is an essential consideration when interpreting imaging data acquired in different postures or translating data acquired in supine imaging to upright function.**

I. Introduction

While computed tomography (CT) imaging is considered the 'gold-standard' in assessing lung structure there are several different imaging modalities that play a significant role in diagnostic chest imaging. For example, magnetic resonance imaging (MRI) is often used to investigate movement of tumors in dynamic sequences that span the whole breath [1], while chest x-ray (CXR) remains a low-cost and low-radiation [2] modality that can be used to track chronic lung disease [3]. Each imaging modality is acquired using different protocols – for example, the lung is typically upright in CXR imaging but supine in CT imaging. Feature mapping between imaging modalities needs to account for lung shape change and lung deformation with posture. Understanding how lung shape change influences tissue distribution in the lung is a challenge due to the non-linear and large elastic deformations that the lung undergoes.

Tomosynthesis provides 3D upright images of the lung in its usual upright functioning posture [4]. Tomosynthesis uses similar ionizing radiation levels to CXR, and can provide limited depth resolution that is absent in CXR [5]. While tomosynthesis is not widely used in chest imaging, it provides an opportunity to assess the movement of the lung tissue between supine and upright postures in 3D space. In this study we present a finite element model of lung tissue mechanics which incorporates lung shape changes between supine and upright postures, which will provide a framework for mapping features between imaging modalities acquired in different postures and for translating data from supine or prone imaging to normal upright function.

This research is supported by a Health Research Council of New Zealand Grant 12/668

H-F Chan, M.H. Tawhai, and A.R. Clark are with Auckland Bioengineering Institute, The University of Auckland, Auckland, New Zealand (corresponding author is A. R. Clark: +64 93737599; e-mail: alys.clark@auckland.ac.nz).

D. Levin and B. Bartholmai are with Department of Radiology, Mayo Clinic, Minnesota, USA.

II. Methods

A. Imaging Data

Volumetric CT (supine) and tomosynthesis (upright) images of the lung were acquired retrospectively from the Mayo Clinic (Minnesota, USA) for five subjects with no pre-existing respiratory disease. Institutional review board approval was granted for the acquisition of the data, and subjects gave informed consent. Images in each posture were acquired from each patient during the same session and were acquired during an inspiratory breath hold.

B. Lung Field Segmentation

The lungs were segmented from the CT images automatically using the custom-built software PASS (Pulmonary Analysis Software Suite, University of Iowa), which provides an automated lung segmentation algorithm [6]. In-house data visualization software (CMGUI, www.cmiss.org/cmgui) was used to render the surface of the lungs, and approximately 20,000 surface coordinates were generated to cover the lung surfaces. A tri-cubic Hermite finite element (FE) mesh was geometry fitted to the lung surface data, as described by Fernandez et al. [7].

The lung was segmented from tomosynthesis imaging using an adaptation of the dynamic programming segmentation method of Wang et al. [8]. Each image slice was cropped using Fiji (fiji.sc/Fiji), an open source image processing software package, such that only the interior of the lungs remained. The cropped images were then resized to ½ the width and ¼ of the height of the original cropped image. This rescaling reduced computational time and the differential scaling of image height and width provided scaled images with a similar height and width. Dynamic programming was employed on the resized images to determine the optimal lung outline through a lowest cumulative cost calculation.

A host mesh deformation was then conducted to transform the supine lung shape to its upright equivalent using CMISS (www.cmiss.org/cm) [7]. This transformation was parameterized by minimizing the summation of the Euclidean distance error between a set of landmark and target points in the supine and upright lungs. Landmark points were chosen at geometrically important locations to represent the lung in the supine posture, while targets were corresponding points that characterized the upright lung.

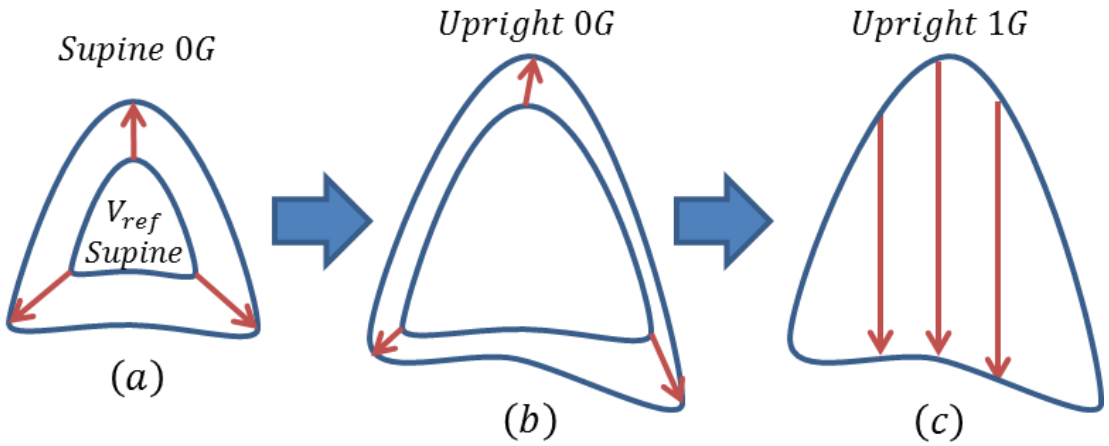

Figure 1: Illustration of the upright lung tissue mechanics simulation. (a) A zero-gravity expansion step from reference volume to the supine lung volume. (b) The supine zero-gravity lung is transformed into the upright equivalent. (c) A full gravitational load is applied in the cranial-caudal direction to simulate lung tissue mechanics in the upright posture

C. Tissue Mechanics Simulations

The deformation of lung tissue under gravity was simulated using a finite deformation elasticity model [9]. In this model the lung was assumed to be a compressible, homogenous, isotropic material with the relationship between stress and strain defined by the strain energy density function (W)

$$W = \frac{\xi}{2}\exp(aJ_1^2 + bJ_2), \quad (1)$$

where J_1 and J_2 are the first and second invariants of the Green-Lagrangian finite strain tensor and ξ, a, and b are constant coefficients. This model was solved by assuming that the lung was free to slide within a rigid pleural cavity under gravity loading with the lung parenchyma remaining in contact with the cavity surface. A theoretical reference volume (a zero stress and strain state) was defined to occur at 50% of the upright lung volume of an individual.

As previous studies have relied on CT imaging to define lung shape, tissue mechanics simulations in the upright posture have assumed isotropic expansion from supine to upright lung volume [9]. In this study, upright lung shape was derived from imaging, so lung tissue mechanics from supine to upright was modified to include a shape change between postures. The reference lung volume was expanded in an isotropic fashion in zero gravity (0G) to supine lung volume (Fig. 1a); the lung was then expanded iteratively in 0G by projecting the supine lung shape to upright lung shape (with the transformation defined by the host-mesh transformation between the two shapes) (Fig. 1b). Then, a gravitational load in the cranial-caudal direction was applied to simulate lung tissue mechanics in the upright posture (Fig. 1c). For each subject, upright lung tissue mechanics was also simulated with the simplified methodology (isotropic expansion from supine to upright lung volume) to determine the effect of shape change on gravitational lung tissue density gradients.

III. Results

A. Lung Shape Changes Between Supine and Upright

Fig. 2 shows an example of the change in lung shape between supine and upright imaging. The upright lung volume was typically bigger than the supine lung volume with an average volume difference of 8.6%, although this difference is not statistically significant (p=0.15). Table I summarizes differences in lung width and height between supine and upright in the five subjects considered.

Analysis of lung dimensions in each found differences in lung height between supine and upright, but smaller changes in lung width and depth. A paired t-test showed that the lung height change between postures was significantly different to the width (medial-lateral) change (p=0.02), and borderline significantly different to the depth (ventral-dorsal) change (p=0.07). The majority of lung height change was in the diaphragm region, and the diaphragm was shown to flatten going from the supine to upright posture. Ventral-dorsal changes were likely due to chest movement.

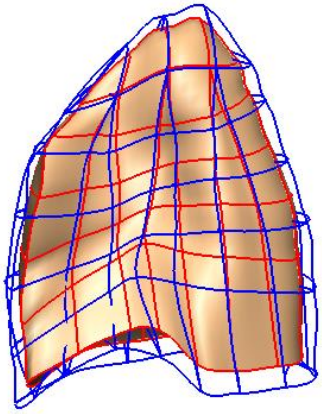

Figure 2: An example of the change in lung shape between supine (solid shape) and upright (wireframe) imaging.

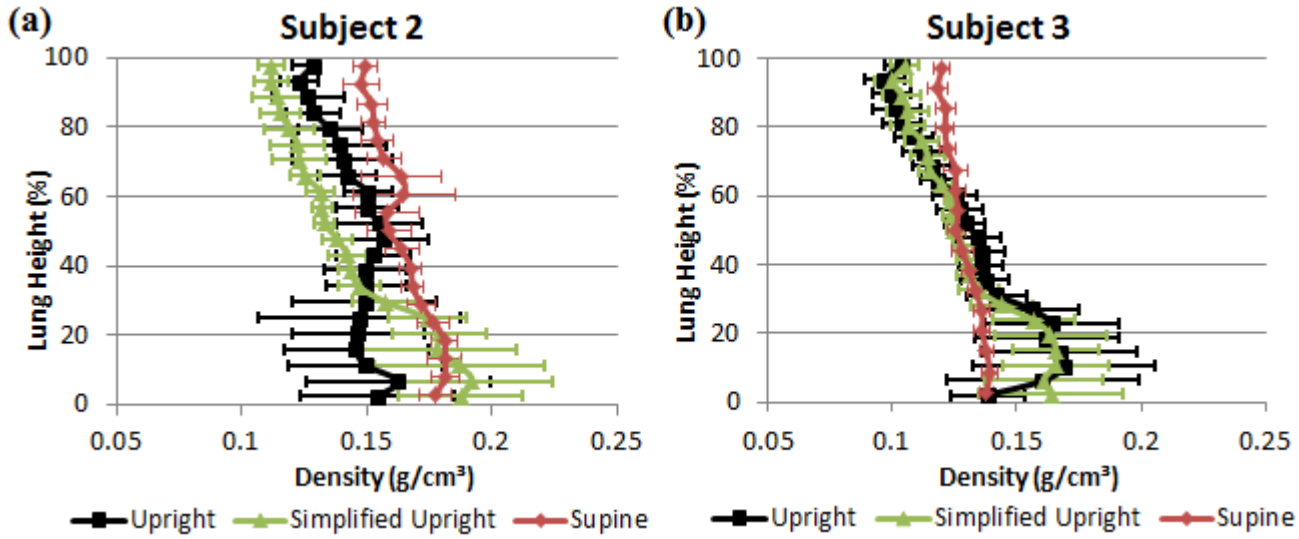

Figure 3: The relationship between density (g/cm^3) and gravitational lung height (%) for supine, upright and simplified upright postures of two subjects. (a) Subject 2 has a different gravitational density gradient between upright and simplified upright simulations due to a large lung shape change between supine and upright postures. (b) Subject 3 however, had very little shape change between postures therefore the upright and simplified upright curves are similar.

TABLE I. CHANGES IN LUNG WIDTH, HEIGHT AND DEPTH FROM SUPINE TO UPRIGHT IN THE FIVE SUBJECTS CONSIDERED.

Subject		Lung Width (medial-lateral)	Lung Height (cranial-caudal)	Lung Depth (ventral-dorsal)
1	Supine	153.0 mm	180.6 mm	119.2 mm
	Upright	156.6 mm	188.1 mm	125.9 mm
2	Supine	185.8 mm	212.8 mm	115.9 mm
	Upright	185.4 mm	221.9 mm	121.6 mm
3	Supine	168.8 mm	242.7 mm	124.3 mm
	Upright	170.8 mm	248.6 mm	123.7 mm
4	Supine	181.3 mm	235.5 mm	154.0 mm
	Upright	182.4 mm	244.9 mm	154.1 mm
5	Supine	170.8 mm	270.7 mm	131.5 mm
	Upright	172.3 mm	271.6 mm	130.7 mm

TABLE II. DIFFERENCES BETWEEN SUPINE LUNG DENSITY AND CT LUNG DENSITY.

Subject	CT Density (g/cm^3)	Supine Density (g/cm^3)
1	0.270	0.269
2	0.162	0.165
3	0.128	0.129
4	0.132	0.132
5	0.134	0.135

TABLE III. DIFFERENCES IN OVERLAP ERROR FOR CT VS. SUPINE AND UPRIGHT VS. SIMPLIFIED UPRIGHT SIMULATIONS IN THE FIVE SUBJECTS CONSIDERED.

Subject	CT vs. Supine Overlap Error *(%)*	Upright vs. Simplified Upright Overlap Error *(%)*
1	3.17	16.62
2	5.18	16.87
3	5.25	3.22
4	5.75	12.66
5	7.61	3.52

B. Lung Tissue Mechanics

Lung tissue mechanics was simulated in the supine and upright shapes and volumes for each subject, and also simplified upright posture (which corresponds to supine lung shape and upright lung volume. Supine lung tissue density gradients were compared against CT imaging data (Table II), and a paired t-test showed no significant difference between measured and predicted values ($p=0.29$). A calculation of the overlapping areas was implemented as a quantification of error between two different density curves. Overlap error calculations were used to compare CT and supine, and upright and simplified upright simulations (Table III).

For every subject, the gravitational density gradient was different between supine and upright simulations. In 3 of 5 subjects the upright gravitational gradients were less steep than their supine counterparts due to higher upright volumes (Fig. 3). In the subjects where there was minimal shape change between supine and upright postures, the upright gradients were similar to the simplified gradients and the overlap error value was small (Fig. 3b and Table III). However, in the subjects where a large amount of shape change occurred between postures, there was a difference in density gradients corresponding to a large overlap error value (Fig. 3a, Table III). Although subject numbers were low there was a significant difference between those subjects with less than 2% volume change between postures (subjects 3 and 5) and those with greater than 2% volume change ($p<0.01$). It can be seen visually (Fig. 3) that upright density gradients seen in these subjects were steeper than their simplified upright equivalents; therefore suggesting a stiffer lung.

IV. DISCUSSION AND CONCLUSION

We have developed a methodological framework for assessing changes in lung shape and predicting lung tissue deformation under gravity in the supine and upright postures Five subjects with imaging, acquired on the same day, from both modalities were selected for this study. The supine lung shape was derived from finite element mesh fitting, and the

upright lung shape from a host mesh deformation. The majority of the shape change between the supine and upright postures was seen in the diaphragmatic region of the lungs.

Lung tissue mechanics was simulated on the two imaging-derived lung shapes to determine whether this shape change corresponded to differences in lung function. Lung tissue mechanics was simulated on the two imaging-derived lung shapes to determine if this shape change corresponded to differences in lung function. Supine density was validated against the gradients seen in CT imaging and upright gradients were predicted using the same tissue properties. The upright gravitational gradients were typically less than their supine counterparts due to higher upright volumes. Simulations were compared to previously-used simplified upright simulations that assumed no shape change between supine and upright postures. In the subjects where there was minimal shape change between supine and upright postures, the upright gradients were similar to the simplified model. However, in the subjects where shape change between postures occurred, there was a significant difference between predictions of upright function.

We show that differences in gravitational density gradients between the postures cannot be explained by volume change alone. In the subjects where there was significant shape change between the supine and upright postures, the upright gradients were steeper than their simplified upright equivalent; this suggested that the lung was effectively stiffer. Our model therefore predicts that shape change is important in the distribution of tissue, and therefore to lung function as tissue deformation plays a role in the distribution of ventilation and perfusion in the lung.

A diaphragmatic change in the lung was also seen in Wade [10], where movements of the diaphragm during respiration were investigated. Wade [10] found that the change from erect to the supine posture caused a larger change in the pattern of movement of the diaphragm and also that diaphragmatic movement occurred even during normal respiration along with chest wall expansion. If these shape changes are significant, the methodology employed here could also be used to better understand the mechanics of respiration and to guide image registration in dynamic imaging of the breathing cycle.

This study lays the methodological groundwork for a validated model of the lung shape change between supine and upright postures in a large population. This modelling framework could be used to constrain image registration between postures and modalities, allowing for long-term monitoring of the lung between postures and imaging modalities.

REFERENCES

[1] N.-Y. Wu, H.-C. Cheng, J. S. Ko, Y.-C. Cheng, P.-W. Lin, W.-C. Lin, C.-Y. Chang, and D.-M. Liou, "Magnetic resonance imaging for lung cancer detection: experience in a population of more than 10,000 healthy individuals," *BMC Cancer*, vol. 11, no. 1, p. 242, Jan. 2011.

[2] C. Schaefer-Prokop, U. Neitzel, H. W. Venema, M. Uffmann, and M. Prokop, "Digital chest radiography: an update on modern technology, dose containment and control of image quality," *Eur. Radiol.*, vol. 18, no. 9, pp. 1818–30, Sep. 2008.

[3] A. M. Speets, Y. van der Graaf, A. W. Hoes, S. Kalmijn, A. P. Sachs, M. J. Rutten, J. W. C. Gratama, A. D. Montauban van Swijndregt, and W. P. Mali, "Chest radiography in general practice: indications, diagnostic yield and consequences for patient management," *Br. J. Gen. Pract.*, vol. 56, no. 529, pp. 574–8, Aug. 2006.

[4] J. T. Dobbins III and D. J. Godfrey, "Digital x-ray tomosynthesis: current state of the art and clinical potential," *Phys. Med. Biol*, vol. 48, no. 19, pp. 65–106, 2003.

[5] J. T. Dobbins III, "Tomosynthesis imaging: At a translational crossroads," *Med. Phys.*, vol. 36, no. 6, p. 1956, 2009.

[6] S. Hu, E. A. Hoffman, and J. M. Reinhardt, "Automatic lung segmentation for accurate quantitation of volumetric X-ray CT images," *IEEE Trans. Med. Imaging*, vol. 20, no. 6, pp. 490–8, Jun. 2001.

[7] J. W. Fernandez, P. Mithraratne, S. F. Thrupp, M. H. Tawhai, and P. J. Hunter, "Anatomically based geometric modelling of the musculo-skeletal system and other organs," *Biomech. Model. Mechanobiol.*, vol. 2, no. 3, pp. 139–155, 2004.

[8] J. Wang, J. T. Dobbins, and Q. Li, "Automated lung segmentation in digital chest tomosynthesis," *Med. Phys.*, vol. 39, no. 2, pp. 732–41, Feb. 2012.

[9] M. H. Tawhai, M. P. Nash, C.-L. Lin, and E. A. Hoffman, "Supine and prone differences in regional lung density and pleural pressure gradients in the human lung with constant shape," *J. Appl. Physiol.*, vol. 107, no. 3, pp. 912–920, 2009.

[10] O. L. Wade, "Movements of the thoracic cage and diaphragm in respiration," *J. Physiol.*, vol. 124, no. 2, pp. 193–212, 1954.